Audio Engineering Society

Conference Paper

Presented at the Conference on
Audio for Virtual and Augmented Reality
2018 August 20 – 22, Redmond, WA, USA

The *SpHEAR project update: the TinySpHEAR and Octathingy soundfield microphones

Fernando Lopez-Lezcano[1]

[1] *CCRMA, Stanford University*

Correspondence should be addressed to Fernando Lopez-Lezcano (nando@ccrma.stanford.edu)

ABSTRACT

This paper in an update of the *SpHEAR (Spherical Harmonics Ear) project, created with the goal of using low cost 3D printers to fabricate Ambisonics microphones. The initial four-capsule prototypes reported in 2016 [1] have evolved into a family of full-featured high quality microphones that include the traditional tetrahedral design and a more advanced eight capsule microphone [2] that can capture second-order soundfields. The project includes all mechanical 3d models and electrical designs, as well as all the procedures and software needed to calibrate the microphones for best performance. A fully-automated robotic arm measurement rig is also described. Everything in the project is shared through GPL [3]/CC [4] licenses, uses Free Software components, and is available on a public GIT repository (https://cm-gitlab.stanford.edu/ambisonics/SpHEAR/).

1 Introduction

The soundfield microphone was designed in the 1970's by Michael Gerzon and Peter Craven [5] to capture the spherical harmonics of a soundfield up to first-order. It uses four capsules in a tetrahedral configuration, which are matrixed and equalized to derive the Ambisonics B-format signals that represent the soundfield. In 2012 Eric Benjamin published the design and evaluation of an eight capsule microphone [2] that could capture second order components.

The goal of the SpHEAR project is to use the advances in reasonably priced 3D printing to build feature-complete multi-capsule microphone arrays that can capture Ambisonics soundfields with increased resolution. Four and eight capsule designs are particularly attractive due to the channel count of current portable sound recording interfaces. The project intends to provide a documented solution that includes 3D models, electrical interfaces and, most importantly, calibration software so that the microphones are usable tools for sound capture, concert and event recording.

In addition to an update to our experiments with the tetrahedral microphone, this paper focuses primarily on the eight-capsule design called the "Octathingy". We present our current approach to derive a successful calibration for it from impulse response measurements.

2 Mechanical design and 3D models

We are interested in mechanical designs that can be printed in low- to medium-price 3D printers, like the Ultimaker 2 Extended [6]. This type of printer uses fused-filament fabrication technology (extrusion) which makes it hard to produce intricate parts with overhangs such as a complete soundfield capsule assembly. In our design, for example, like in the original SoundField microphone, each capsule holder is a separate part that is later assembled into a complete array.

In our current microphones the three main 3d printed parts (two flares and the body, see figure 2) hold the interface printed circuit boards and connect to the capsule array on one end and a suitable connector on the other. Windscreen and shock mounts can also be 3d printed and added to the microphone.

Subtle details of the design are beyond the scope of this article, but a lot of thought and much experimentation has gone into designing parts that can be easily printed and assembled together. All 3D models are written in OpenSCAD, a constructive solid geometry (CSG) 3D modeling environment based on a functional programming language [7], chosen for its flexibility and open nature.

2.1 TinySpHEAR, the tetrahedral design

The prototype described in the original paper was a simple design with minimal interface electronics that exhibited poor noise performance at low frequencies. The next prototype, built with 10mm Primo EM182 capsules and an array radius of 9.2mm in August 2016, used the Zapnspark [8] active balanced phantom power circuit derived from the well known Schoeps circuit, and exhibited much better performance. The next microphone was built with 14mm Primo EM200 capsules and an 11mm array radius, and was finished in February 2017. The 14mm capsules, used for this and subsequent microphones, exhibit much better performance below 1KHz, and do not need as much equalization to acquire a flat frequency response as the 10mm capsules do.

A variant of the same mechanical design was designed as a custom modification to a Zoom H2N four channel recorder, replacing the four internal capsules with an external tetrahedral array.

The current prototypes add threading to the body so that a 3d printed windscreen assembly can be attached to the microphone. The windscreen has a foam insert for low wind conditions and a fake fur cover for high wind conditions. The microphone slides into a shock mount that can be mounted on a conventional microphone stand (see figure 1).

Fig. 1: TinySpHEAR and Octathingy microphones

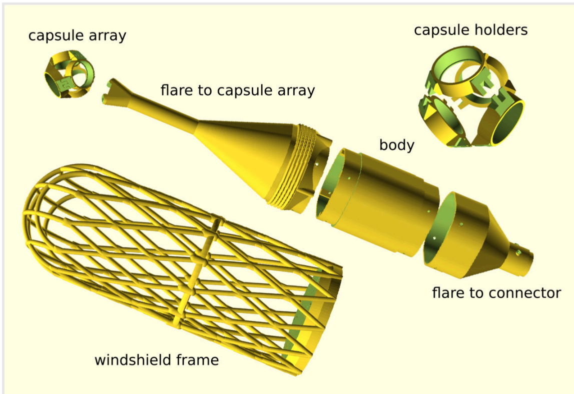

Fig. 2: TinySpHEAR 3d models

2.2 The OctaSpHEAR / Octathingy

The OctaSpHEAR is the physical realization of the Octathingy, an eight capsule design by Eric Benjamin [2]. The Octathingy can capture second-order soundfields, and also provides better first-order performance. The first prototype was finished in June 2017 (version 1, v1 for short). Its mechanical design is an extension of the tetrahedral microphone and includes eight phantom power interfaces and a DB25 connector. The second prototype, with the same capsule array design and capsules angled to the same elevation as the tetrahedral design (35.26 degrees from the horizontal plane) and with an array radius of 16.6mm was finished in April

2018. A third was built recently with a modified capsule array configuration (version 2, or v2 for short, see section 6), but regretfully not in time for a detailed analysis to be included in this article.

3 Measuring the SpHEAR microphones

Another part of the project is the design of a system that can measure the microphones with enough accuracy for an effective calibration. This has proven to be as much of a challenge as the microphones themselves.

3.1 Measurement rig

For recovery and calibration of horizontal spherical harmonics it is sufficient to use horizontal-only measurements. We also use horizontal-only measurements for calibrating the tetrahedral design because we assume that, due to its symmetry in all axes, behavior in the Z-direction is roughly the same as in the X and Y directions.

Designing a measurement setup for horizontal-only measurements can be done relatively easily. In our case, we built a rotating table that includes an adjustable height microphone holder with a small X-Y table at the bottom to precisely align the center of the microphone with the center of rotation of the table.

Calibrating spherical harmonics that have nulls in the horizontal plane in the eight capsule design requires additional measurements above and below the horizontal plane, as symmetries can no longer be used to approximate these harmonics from others.

A redesign of our rig allowed it to tilt, making measurements with elevation possible. A better alternative was desired that would give us speed, precision and repeatability in the measurement process.

3.1.1 Current measurement hardware

Our current fully automated measuring system is based on the the WidowXL kit from Trossen Robotics, a small 5-degree-of-freedom robotic arm. Its cost, around $2500 (with an additional servo), which falls within our budget. It can hold 500g at maximum reach — our heaviest 8 capsule microphones weight is under 200g — and has servos with 4096 point resolution.

The goal of the system is to rotate the microphone around the center of its capsule array, achieving full 360-degree azimuth rotation and as much elevation range as possible. The length of the arm segments, the rotational limits of its servos and the length of the microphone define the geometrical constraints that limit which angles can be reached.

Although we started using the stock arm, we made a few hardware changes to optimize it for our purposes. The wrist-rotation servo and the gripper assembly with its servo were replaced with a single servo that can rotate 360 degrees (the stock servos in those joints have a limit of 300 degree rotation). This minimizes the distance between the wrist joint and the center of the capsule array, which directly affects the reach of the arm, and allows the wrist to rotate a full 360 degrees for full azimuth measurement coverage.

A small 3d printed plate is attached to the wrist rotation servo and includes sockets that allow different microphone assemblies to be easily plugged in for measurement.

We have found two useful poses of the arm. In both of them we avoid using the servo that rotates the arm on its vertical axis so that the arm always lies in the same plane as the microphone and speaker and does not significantly change its profile and reflections during the measurement process. In the first pose (figure 3) the center of the microphone array is held over the rotational center of the arm and the arm is used to tilt it to achieve symmetrical elevation changes.

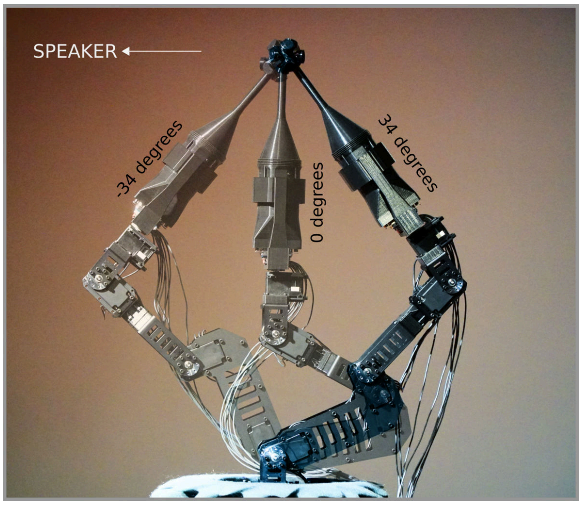

Fig. 3: Three positions of the arm, centered mode

In the second pose (figure 4) the center of the microphone array is offset from the center of the arm towards the speaker. The center of the capsule array can be lower, so the pose allows more coverage of the upper hemisphere and correspondingly less of the lower hemisphere.

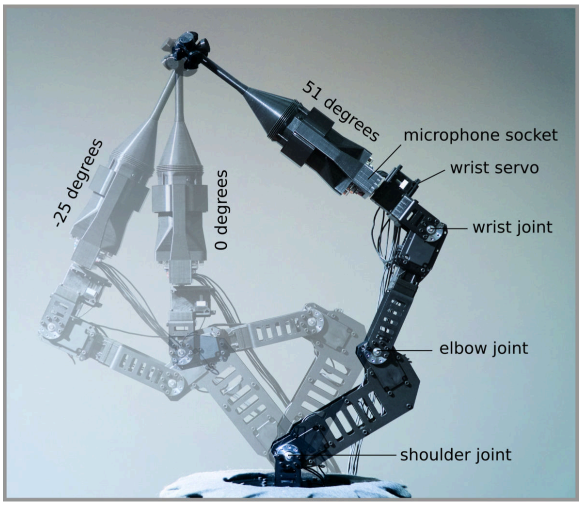

Fig. 4: Three positions of the arm, offset mode

With a distance between the wrist joint and the center of the array of 357mm, and using the offset pose, the modified arm can tilt the microphone up to +51 degrees and -25 degrees from the horizontal plane. With the same conditions and the centered pose the reach is +/- 34 degrees of elevation. The unmodified arm reach is about 14 to 16 degrees less under the same conditions.

3.1.2 Current measurement software

The arm has an Arduino based built-in control processor with a serial interface, and firmware that can move the arm in different modes, but its inverse kinematics equations are designed to only handle the stock arm with its gripper assembly. The firmware also has built-in rotational limits for the servos that are unnecessarily conservative and limit the reach of the arm.

We use the arm control firmware in its "backhoe mode", in which it receives raw servo rotation numbers, and implement our own inverse kinematics code [9] externally. We modified the firmware to take into account the changed wrist rotation servo, and also adjusted the servo rotation limits to safe but wider ranges, maximizing the reach of the arm.

We implemented the measurement control software in SuperCollider [10] as it can easily handle playing back and synchronously recording the sine sweeps used to measure the impulse responses, and also control the arm through its serial interface. The inverse kinematics equations output the correct servo rotation values for the arm given the coordinates of the center of the microphone and the desired azimuth and elevation angles of the measurement, and an interface layer communicates with the arm firmware using its control protocol. The software can also automatically determine the optimum values of the height and offset of the capsule array to maximize the elevation reach of the arm for each pose (angles are rounded to the next degree, distances to multiples of 1mm).

A measurement run is a loop that iterates over the requested measurement angles, playing a sine sweep and recording the output of all capsules, then moving the arm to the new position and waiting for it to stabilize before starting with the next measurement.

3.2 Measuring techniques

Since an anechoic room is not available, all measurements use pseudo-anechoic techniques [11] and the biggest space we have (the dimensions of the space determine the maximum length of the direct path that we can record). Our small concert hall (the Stage) enables us to capture usable impulse responses of up to approximately 4.5 mSecs, which translate into a low frequency measurement limit of around 220Hz. The excitation source is an K&H M50 single driver speaker with a frequency response of 100Hz to 20KHz +/- 5dB, and an EMM-6 microphone is used as a calibration reference.

For calibrating the microphones we need to capture impulse responses equally spaced around the capsule array so that they sample the spherical harmonics we want to encode. For horizontal-only measurements of a first order component we need a minimum of 4 equally spaced measurements, but we use 8 for robustness. For second order components we need twice that number. For full 3d measurements we want a set of points lying on the surface of a sphere that optimally sample the harmonics.

A set of N points on the surface of a sphere is called a spherical t-design [12] if the integral of any polynomial of degree at most t over the sphere is equal to the average value of the polynomial over the set of N points. A spherical t-design optimally samples our harmonics, so we select one that provides a similar density of measurements to the one we are using in the horizontal plane.

A 180-point t-design has 16 points lying within the +/-5 degree elevation band (or 28 points within +/-10 degrees of elevation) and is considered satisfactory. Since the robotic arm cannot reach all elevation angles, only a subset of those points will be measurable. For the example shown above, (offset coverage from +51 to -25 degrees in elevation) 108 points of the 180 are reachable. A measurement run of this subset of the 180 point t-design using 10 second sine sweeps takes approximately 40 minutes.

We use the substitution method — an omnidirectional calibrated microphone (EMM-6) located in the same spatial coordinates as the microphone under calibration — to record a reference impulse response and calculate an inverse filter for the speaker response using the DRC (Digital Room Correction) [13] software package. All captured impulse responses are convolved with this inverse filter. The equalized impulse responses are then trimmed to isolate the direct path from all reflections of the room, and windowed with a Blackman window centered on the impulse. The Blackman window provides empirically better ripple in the passband, which translates to flatter response at low frequencies, than other alternatives we tried (for example a Tukey window).

4 Calibration

4.1 TinySpHEAR calibration

The calibration procedure for the tetrahedral microphone described in the previous paper [1] created a 4×4 matrix of FIR filters. The filters were the result of merging a low and mid frequency matrix of filters calculated using singular value decomposition in logarithmically spaced frequency bands, with four filters that equalized the B-format signals in the high frequency range. This approach was unnecessarily complex, was simplified early on, and the calibration currently uses the same procedure outlined by Gerzon in his seminal paper [5].

The frequency response of the recorded impulse responses is used to select a frequency range in which the microphone acts as a colocated array, and a static A-to-B format 4×4 matrix is calculated in that range by singular value decomposition [14]. The A-format calibration impulse responses are then converted to B-format using this matrix, and four FIR filters are derived from the magnitude spectrum response of the resulting B-format signals. These filters try to correct the response of the microphone at high frequencies, and also compensate for the low frequency response of the capsules, if needed. Converting those filters to minimum phase gives us the proper phase response, and the B format polar plots maintain their shape and orientation over the full frequency range of the microphone. The final encoder consists of the A-to-B matrix and four FIR filters, and is written out as a Faust program that can be compiled to multiple plugin formats.

4.2 Octathingy calibration

The calibration of the Octathingy eight capsule microphone was approached as an extension of the procedure outlined in the previous paragraph, and initially consists of a static A-to-B encoder matrix derived for a frequency range where the capsules are co-located (below about 2.5KHz in our prototypes), followed by one correction filter for each component of the B-format signal set. Of the nine second-order spherical harmonics the capsule array can successfully sample only eight, as “R” aliases to “W” and cannot be extracted independently.

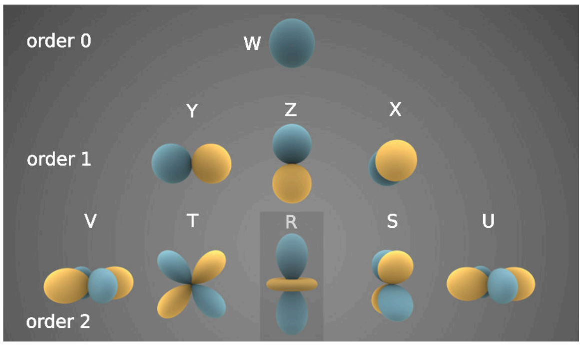

Fig. 5: 2nd order spherical harmonics[1]

The second-order components of an open array made of cardioid capsules are difference microphones [15]. As such there are practical problems in recovering those harmonics at both ends of the audio spectrum. Their output level decreases with decreasing frequency at a rate of 6dB/oct, so at low frequencies the self noise of the capsules limits the maximum gain that can be applied to compensate for the drop, and imposes a low frequency limit that is higher than the low frequency response of the capsules. At high frequencies, spatial

[1] https://commons.wikimedia.org/wiki/File:Spherical_Harmonics.png

aliasing takes place and the components are no longer spatially correct, for our array radius of 16.6 to 18mm the effects start happening at around 9.5-10KHz.

Furthermore, difference microphones are more sensitive to small differences in capsule gain and polar pattern and to the precision of the geometry of the array. Any mismatches will introduce errors in the recovery of the harmonics. Physically matched capsules, especially with regards to polar pattern, are a good start, but equalizing the capsules using the measured impulse responses improves the recovery of the second-order harmonics.

A practical consideration arises, which is what impulse responses to use for the individual capsule inverse calibration filters. It is essentially the same issue that will arise later when we have to decide how to optimize the B format compensation filters. In both cases, a reasonable assumption is to favor the horizontal plane and low elevations, which is the most likely region to be of importance in real life concert or music recordings.

This is not, of course, the only possible approach. For example, in our concert recordings, our capture microphone is usually hanging upside down and elevated from the plane of the audience and potential musicians. A more useful approach in this case would be to calibrate the microphone so that the best frequency response and spatial clarity occurs in the direction of a cone pointing slightly "upwards" (from the point of view of the microphone), and at an elevation angle of 10 or 20 degrees. Other use cases are possible.

In this paper, we present the optimization for the horizontal plane, so the initial calibration of the capsules will be done through measurements in that region of the sphere. These filters will make the capsule frequency response in the horizontal plane flatter, but most importantly, all the capsules will be closer to each other in response.

The equalized A-format horizontal plane capsule signals are used to create a subset (8×5) of the full 8×8 A-format to B-format conversion matrix by singular value decomposition in a frequency range where the capsules behave as if they were co-located (800Hz to 1600Hz in these examples). The matrix is then used to create a first generation of partial B-format signals (W/X/Y/U/V) derived from the equalized A-format signals. The B-format signals will be correct up until the transition frequency of the array, where the capsules can no longer be considered co-located. The observed transition is about an octave below the limit frequency of 6.5 kHz calculated using Gerzon's approximate formula for our array radius of 16.6mm. Figure 6 shows the combined effects in the high frequency region of the non coincidence of the capsules and the resonance of the space enclosed by them (see figure 18).

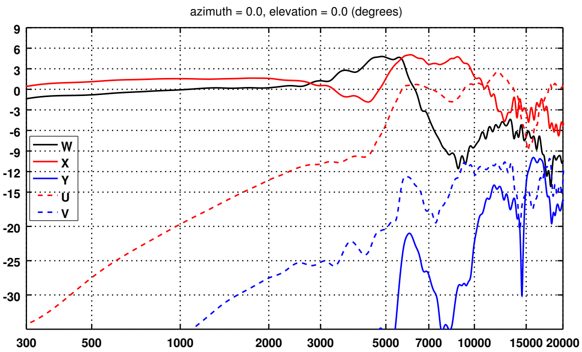

Fig. 6: Octathingy B format frequency response for static A to B matrix only

Note the 6dB/oct drop in the second-order U/V components. Like in the case of the tetrahedral microphone, we extract the magnitude spectrum response of each component and use it to derive an inverse filter that will try to correct for the high frequency problems (figure 7).

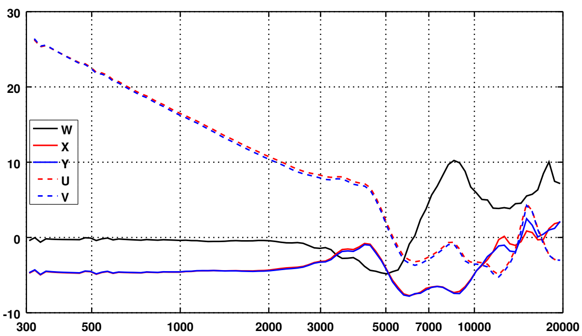

Fig. 7: Octathingy B format equalization filters, horizontal plane measurements

The second order filter automatically includes the 6dB/oct filter needed to compensate for the low frequency loss of the difference microphones.

We can now generate corrected B-format signals from the A-format capsule signals, first routing them through the capsule equalization filters, then through the static

8×5 matrix, and finally through the B-format equalization filters. This will generate horizontal B-format components that have been optimized for the horizontal plane. Figure 8 shows the equalized horizontal first and second order components. For 0 degree incidence angle, W, X and U have maximum amplitude, while Y and V have nulls. Note that Y's null is affected at high frequencies while V's null is less pronounced at all frequencies.

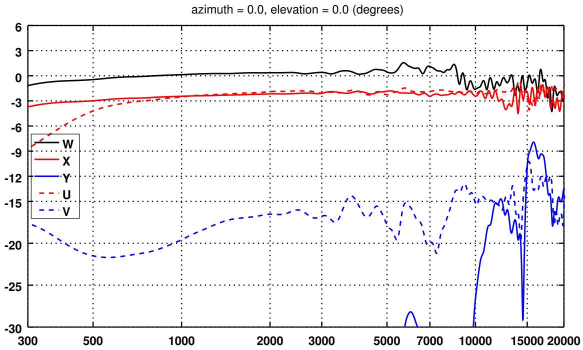

Fig. 8: Octathingy B format frequency response for matrix and filters, horizontal plane measurements

We now repeat this process using the full 3D set of measurements instead of the horizontal plane measurements and generate the missing Z/S/T components. Our final hybrid 8×8 A-to-B matrix and 8 B-format filters are a mix of the two, each harmonic optimized for an area of the sphere.

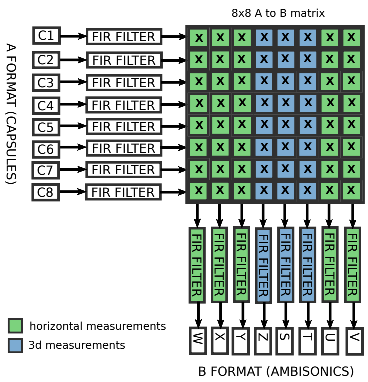

Fig. 9: 2nd order A to B encoder

Figure 10 shows the hybrid B format equalization filters. Figure 11 shows the B format frequency response of all B format components for 0 degrees azimuth and elevation, both Z and S, and to a lesser extent T have low values (they should be null).

Figure 12 shows the same, but for 48 degrees elevation. There are problems in the horizontal B format components at high frequencies. The encoder for those signals was generated from horizontal-only measurements and they are affected because the response of the capsules has changed due to the change in elevation while the filters have not.

At this point the calibration is finished and a complete encoder can be created from the 16 FIR filters and A-to-B matrix. An example implementation can be written out as Faust code, which can subsequently be compiled to a number of plugin formats.

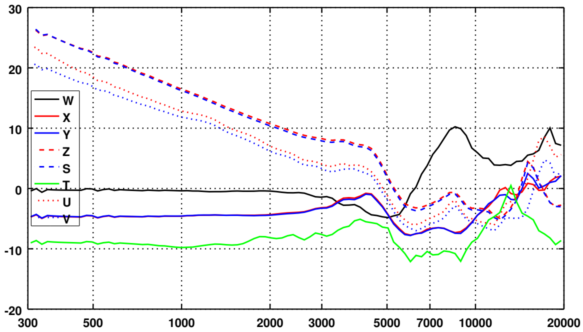

Fig. 10: Octathingy B format equalization filters, full 3d

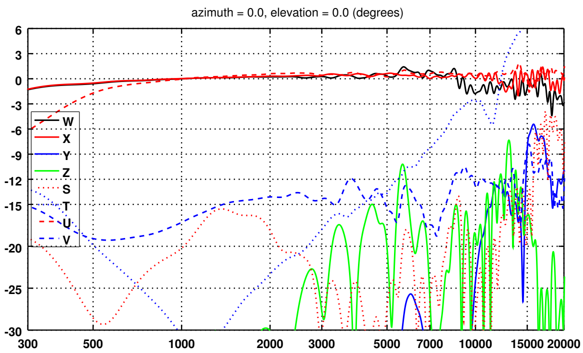

Fig. 11: Octathingy B format frequency response, 3d, 0 degree elevation

Figures 13, 14 and 15 show the polar response of each of the spherical harmonics at mid and high frequencies. All plotted points come from the t-design set, so they are not necessarily equally spaced. The black dots show the theoretical value of the spherical harmonic, the red dots the measured value.

Another perspective on the performance in first order of the Octathingy is this pair of graphs (figure 16 for the

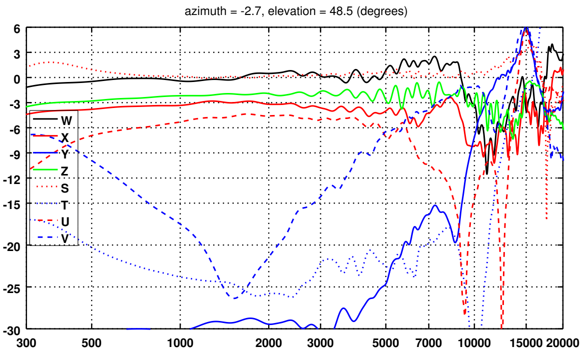

Fig. 12: Octathingy B format frequency response, 3d, 48 degrees elevation

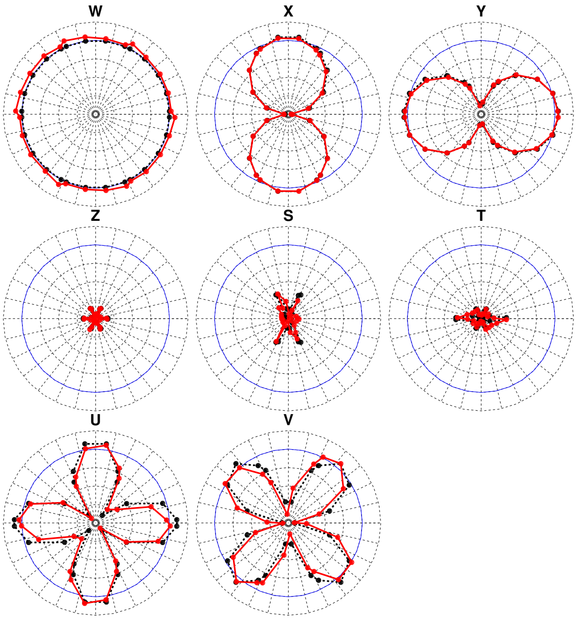

Fig. 13: Polar response of spherical harmonics, t-design points between -10 and +10 degrees elevation, 1.7KHz

Octathingy and 17 for the TinySpHEAR). They show the upper frequency range and the first order horizontal component frequency response in the cardinal (0, 90, 180, 270 degrees, solid lines) and diagonal (45, 135, 225, 315 degrees, dashed lines) directions for both W and X/Y (these measurements were taken under the same conditions). They illustrate how the Octathingy shows a more even frequency response in the higher frequencies, without the pronounced drops in response that naturally occur in the tetrahedral design due to the distortion at high frequencies of the polar pattern of the capsules (the tetrahedral calibration for this graph was done by averaging the cardinal directions).

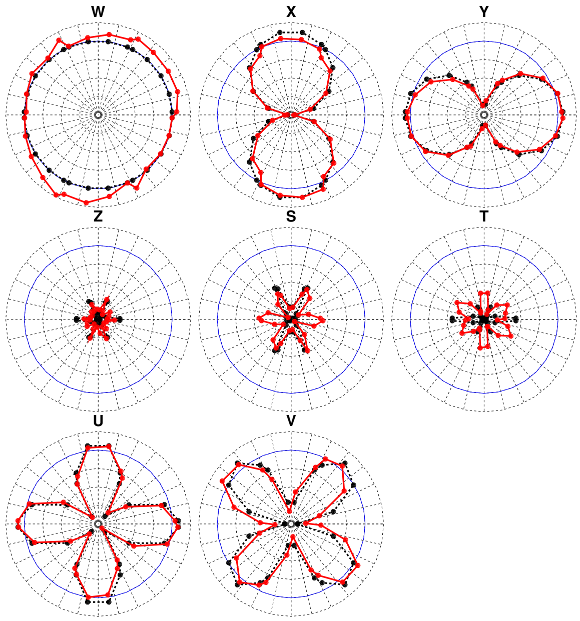

Fig. 14: Polar response of spherical harmonics, t-design points between -10 and +10 degrees elevation, 7KHz

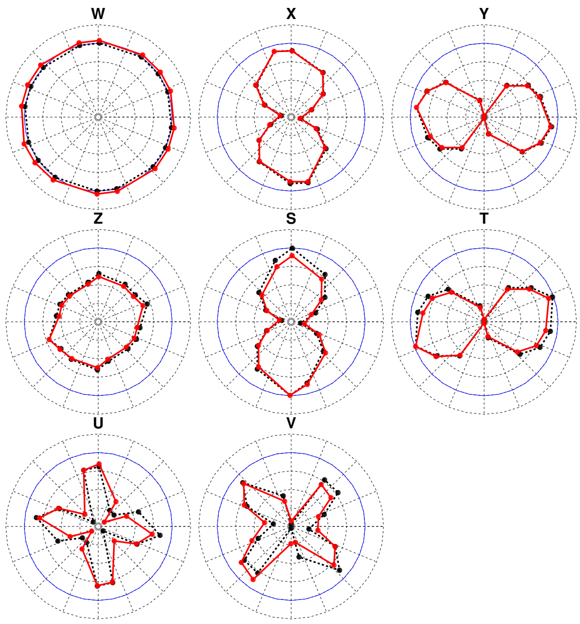

Fig. 15: Polar response of spherical harmonics, t-design points between 25 and 35 degrees elevation, 1.7KHz

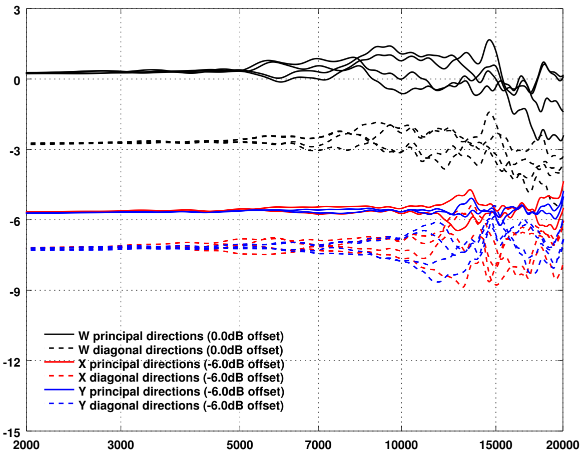

Fig. 16: Octathingy 1st order cardinal and diagonal responses

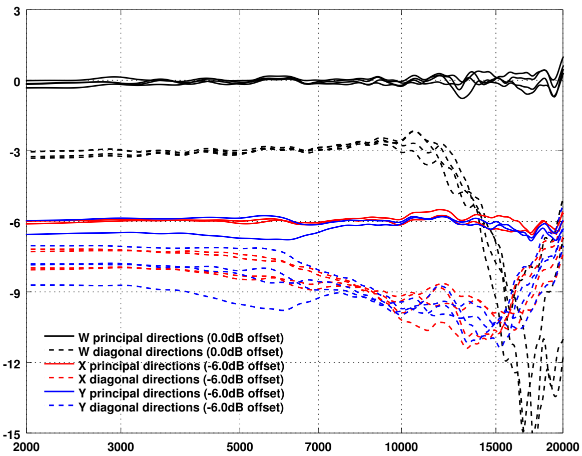

Fig. 17: TinySpHEAR 1st order cardinal and diagonal responses

5 Second order components and capsule self noise

The drop of 6dB/oct of the output of the second-order components with decreasing frequency means that the self-noise of the capsules imposes a low frequency limit in the response, otherwise the signal-to-noise ratio of the microphone will suffer adversely. In our prototypes we can get usable output down to about 400Hz, but the necessary amplification, even when limited, creates audible noise for very quiet recordings.

Our proposed workaround is to route the second-order components through an expander so that, at a programmable level (-45dB by default) the expander starts attenuating the second-order signals (together with the noise).

At very low levels, the background noise is eliminated and the microphone only outputs first-order components. The loss in spatial resolution at very low signal levels is completely acceptable as it eliminates the noise in very quiet segments of the recording or silences.

The expander can generate artifacts (noise pumping), so it is possible to bypass it when the materials being recorded are affected. This is all done after the recording is made so tests can take place to decide which are the best expansion settings for a particular recording.

6 Capsule behavior in the array

While investigating the individual capsule equalization filters it became apparent that the mechanical design of the Octathingy version 1, which was a simple extension of the 3D model originally created for the tetrahedral design, was not optimal in terms of its acoustic behavior. The eight capsules enclose a cavity which acts as a Helmholtz resonator and distorts the frequency and polar response of the capsules. The measured frequency of the resonance (around 4KHz in our prototype) closely matches the size of the cavity.

The effect of the resonance and the shadowing effect of all capsules on each other distort the capsule polar patterns, making them more omnidirectional in the resonant frequencies.

Figure 18 shows the frequency response of one capsule as a function of incidence angle of the signal. The front to back ratio of the capsules at around 1KHz is about 25dB, while at 4KHz it drops to about 8dB. Figure 19 shows the polar pattern of the cardioid capsule becoming more omnidirectional at the resonant frequencies.

It is worth mentioning that this effect also happens in the tetrahedral design, but as the array radius is smaller, the frequency of the main resonance is higher (around 6KHz for an array using 14mm capsules, even higher for 10mm capsules).

As a result of this observation a different mechanical design was created (version 2, figure 20) in which each capsule is housed in a conical vented holder, all eight attached to a central spherical hub that maintains the precise capsule orientation required.

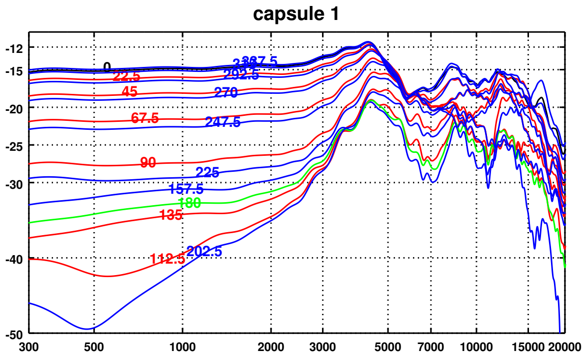

Fig. 18: Octathingy v1 capsule frequency response as a function of incident angle, as indicated on the corresponding trace (in degrees)

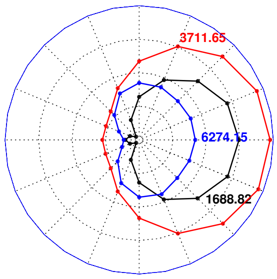

Fig. 19: Octathingy v1 capsule polar patterns at different frequencies

Fig. 20: Octathingy v1 and v2 capsule arrays

Figure 21 shows the frequency response and figure 22 the polar response of one capsule for horizontal plane signals coming from 16 separate equally spaced directions for the new capsule array design.

Each capsule now has a much smaller resonating cavity behind it, with a higher resonant frequency than before, and capsules are isolated from each other. The vents around the holder were made as big as possible to minimize the interference with the capsule's polar response, and still have a mechanically robust array.

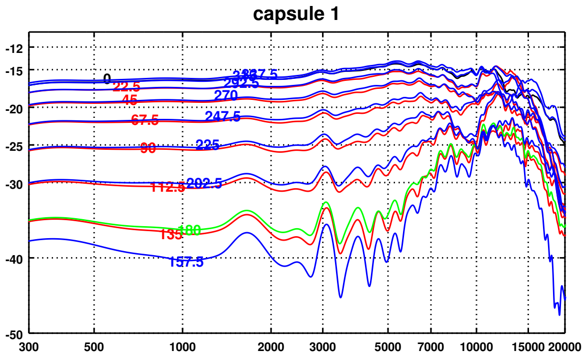

Fig. 21: Octathingy v2 capsule frequency response as a function of incident angle

The spherical core is also as small as possible, and that is the reason why the holders are conical.

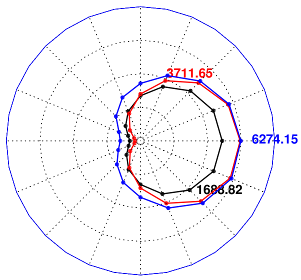

Fig. 22: Octathingy v2 capsule polar responses at different frequencies

The capsules work as cardioids at higher frequencies than before, but this design also affects the polar patterns of the capsules below 1KHz. The physical construction of an array with this design leads to a bigger microphone radius than before, and that implies a lower transition frequency for the microphone, but the difference is small and probably offset by the better performance at high frequencies.

We have not been able to do a full analysis of the microphone that uses this array in time for publication.

7 In the field

Both designs (tetrahedral and eight capsule) have been used for field recordings and for recording concerts and events here at CCRMA. Recordings ranged from cello performances, in which informal subjective tests have compared them favorably with much more expensive commercial microphones that were used side-by-side, to concert recordings that captured varied performers

Fig. 23: recording studio, field recordings, concerts

and styles, from solo acoustic instrument recitals to full 3D surround fixed media and mixed media pieces.

Both microphones have been used extensively over the past year to record first and second order sound materials for the creation of two electroacoustic compositions by the author of the article. The recordings included capturing the sound and space of the detuned strings and soundboard of two discarded pianos[2], and recordings of cello sounds being piped through the soundboards of the pianos. The built-in space of the recordings was presented directly, and also modified through soundfield manipulation techniques. Both pieces are mixed order, with layers created using 5th and 2nd order Ambisonics, and were premiered in concert in October 2017 for the inauguration of our 56.8 HOA (High Order Ambisonics) diffusion array in our Stage concert hall. The cello piece[3] was written for and performed by Séverine Ballon.

8 Conclusions

The project has been successful in creating an open design for Ambisonics microphones that can capture soundfields of up to second order. The current calibration protocols, while experimental, have produced A format to B format encoders that have good performance, both objectively and also subjectively through informal listening tests.

[2]https://ccrma.stanford.edu/ nando/music/como_arpa_vieja/
[3]https://ccrma.stanford.edu/ nando/music/multiplication_of_strings/

In the particular case of the Octathingy, we have shown that an extension of the simple calibration procedure used for the tetrahedral microphone can be used for deriving second order components as well. The frequency response and polar patterns of the recovered B-format signals are good, only showing significant deviations from a flat frequency response and the correct polar pattern shapes above 9 to 10KHz. Simulated first-order cardioid and second-order lobes maintain their shape and direction over the full range of frequencies of the microphone. Furthermore, current 3D printers can fabricate second order arrays that are accurate enough to show good performance.

An automated measurement system has also been presented that simplified the tedious task of capturing large number of impulse response measurements precisely and in a repeatable way.

9 Further work

The automated measurement system can use improvements, in particular we would welcome more elevation coverage for better characterization of our designs. Since the weight of our microphones is less than the maximum carrying capacity of the arm, we are planning on extending its shoulder and elbow segments to increase the elevation reach of the arm.

Further work is also needed to fine tune the mechanical and acoustical design of both microphones, and to continue our work on improving the calibration procedure we need to find ways in which we can objectively characterize A to B format encoders.

A preliminary comparison of the two capsule array physical designs of the Octathingy (v1 vs. v2) show surprisingly small differences in the errors of the recovered B-format signals, even though there are big differences in the capsule signals. A more detailed examination of the results needs to be done before we can draw conclusions.

The project would benefit from a free software feature-complete encoder plugin, as well as a stand-alone microphone processor that can handle both the tetrahedral and the 8 capsule designs, similar in functionality to Fons Adriaensen's TetraProc [16]. We plan to expand the existing example Faust plugin, as well as considering other portable platforms for implementation.

10 Thanks

Special thanks to Francois Germain for many hours of listening to my thoughts and a very thorough critique and review of this article, it is much better thanks to him. Thanks to Chris Chafe and Elliot Kermit-Canfied for independently suggesting we use a robotic arm for the measurement process, and reviewing the paper, and to Aaron Heller and Eric Benjamin for listening to long email threads over a very long time, and providing thoughtful advice and encouragement.

This project would not have been possible without the support of CCRMA at Stanford University, its fantastic research environment, and the fabrication facilities of the MaxLab.

References

[1] Fernando Lopez-Lezcano, "The *SpHEAR project, a family of parametric 3D printed soundfield microphone arrays", AES Conference on Sound Field Control, July 18–20 2016, Guildford, UK

[2] Eric Benjamin, "A second-order soundfield microphone with improved polar pattern shape", Audio Engineering Society Convention Paper 8728, 133rd Convention, San Francisco, 2012

[3] Free Software Foundation, GNU General Public License, http://www.gnu.org/licenses/gpl-3.0.en.html

[4] Creative Commons, CC Attribution-NonCommercial-ShareAlike 4.0 International, http://creativecommons.org/licenses/by-nc-sa/4.0/

[5] Michael Gerzon, "The Design of Precisely Coincident Microphone Arrays for Stereo and Surround Sound", 50th Audio Engineering Society Convention, Preprint L-20, London, 1975

[6] Ultimaker 2 Plus Extended 3D printer, https://ultimaker.com/en/products/ultimaker-2-plus

[7] OpenSCAD, The Programmers Solid 3D CAD Modeller, http://www.openscad.org/

[8] Zapnspark, "Generic Back Electret Condenser Microphone", http://www.sdiy.org/oid/mics.html, 2007

[9] Serdar Kucuk, Safer Bingul, "Robot Kinematics: Forward and Inverse Kinematics", Industrial Robots Theory, Modeling and Control (Chapter 4), 2006, edited by Sam Cubero, ISBN: 3086611-285-8

[10] SuperCollider, https://supercollider.github.io/

[11] Eric Benjamin, "Extending Quasi-Anechoic Electroacoustic Measurements to Low Frequencies", Audio Engineering Society Convention Paper 6128, 117 Convention, San Francisco, 2008

[12] R. H. Hardin and N. J. A. Sloane, "McLaren's Improved Snub Cube and Other New Spherical Designs in Three Dimensions", Discrete and Computational Geometry, 15 (1996), pp. 429-441

[13] Denis Sbragion, DRC (Digital Room Correction), http://drc-fir.sourceforge.net/

[14] Aaron Heller, "Derivation of the A-to-B matrix for a coincident array of first-order microphones", unpublished, 2007

[15] Peter Plessas, "Rigid Sphere Microphone Arrays for Spatial Recording and Holography", Diploma thesis in Electrical Engineering - Audio Engineering, 2009, IEM Institute of Electronic Music and Acoustics University of Music and Performing Arts Graz, Austria

[16] Fons Adriansen, "A Tetrahedral Microphone Processor for Ambisonic Recording", Linux Audio Conference 2007, TU Berlin, Germany

[17] Aaron Heller, Eric Benjamin, "Calibration of Soundfield Microphones using the Diffuse-Field Response", Audio Engineering Society Convention Paper 8711, 133rd Convention, San Francisco, USA